Differences In Cortical Pore Morphology In Regions Of Tension And Compression In The Femoral Diaphysis

Mikayla R. Hoyle[1], Mariana E. Kersh[1, 2, 3]
[1]Dept. of Mechanical Science and Engineering, [2]Beckman Institute for Advanced Science and Technology, [3]Carle Illinois College of Medicine, University of Illinois Urbana-Champaign, Urbana, IL
mrhoyle2@illinois.edu

Disclosures: Mikayla R. Hoyle (N), Mariana E. Kersh (N)

INTRODUCTION: Bone mechanical function is related to cortical microstructure and has important implications for improving the diagnosis of poor bone quality by incorporating measures of pore morphology. The mechanical properties of bone are spatially heterogeneous and may be related to the habitual loading environment of long bones resulting in regions of tension and compression[1,2]. However, there are inconsistent reports on whether cortical pore microstructure varies by anatomical location[6-8]. Moreover, while intuitive, cortical pore measures were adapted from trabecular bone but may not fully capture differences in cortical structure. Therefore, the aim of this study was to evaluate cortical pore morphology in regions known to be loaded in tension or compression using canonical and alternative metrics of pore structure. We hypothesized that loading condition will result in different pore morphologies.

METHODS: Mechanical loading of cortical bone during walking was evaluated using previously developed muscle-driven finite element (FE) models[9]. Six models were used to analyze principal strains and identify regions of tension and compression (Abaqus 2020). The resulting strain maps guided extraction of cadaveric bone samples from the femoral diaphysis (ages = 65,71; female, Fig 1B). Bone samples (n=6 compression, n =5 tensile, nominal dimensions = 16.8 mm² x 5.0 mm) were machined under water irrigation and micro-computed tomography (μCT) data (isotropic resolution = 5.3 μm, Rigaku CT Lab HX130) were acquired. The μCT images were filtered using a non-local means filter (Matlab 2021a), binarized (Fiji), and skeletonized (Amira, 2022.2, Fig 1B). We identified alternative measures of pore morphology by reviewing how network-like structures have been characterized in other fields (e.g., trees, veins/arteries, and fault lines)[10-14]. For each sample, cortical pore measurements were obtained (Amira 2022.2, Fiji, BoneJ, Table 1). Normality of data was confirmed using a Shapiro-Wilk test and statistical outliers were removed to evaluate the differences in pore structure (t-tests, $p < 0.05$).

RESULTS: During walking, maximum tensile principal strains were on the lateral aspect of the diaphysis while maximum compressive strains were on the medial aspect (Fig 1A). Of the classical measures, canal orientation and tortuosity were different in regions of tension versus compression (Table 1). In tensile regions, canal orientation was 26.6% higher (more vertical, Fig 2A) and canal tortuosity was moderately increased (0.38%, Fig 2C) compared to compressive regions. While not significant, there was a difference in the prevalence of large pores: regions of tension had a 51% increase in large pores compared to compressive regions (Fig 2D). Of the new measures, the variability of the canal rotating angle (a measure of canal direction in the plane orthogonal to the long axis) was 20.3% higher in tensile regions compared to compressive regions (Fig 2B).

DISCUSSION: The results support our hypothesis and suggest that bone typically loaded in compression is more structured and follows the classic depiction of the pore network as straight (less tortuous) and vertical (lower orientation angle) canals, while the pore network of bone in tension may be less structured. Others have also reported differences in canal orientation and tortuosity between anatomical regions in rodents[15,16,2]. The less organized network of bone under tension may result from increased variation in local strains that elicit different remodeling responses[17]. Increased prevalence of large pores has been linked to aberrant remodeling of bone where cutting cones merge to create large pores that fail to complete remodeling. To our knowledge, deviation of the canal rotating angle and prevalence of large pores has not been compared between anatomical regions and our results may highlight their use as a biomarker of loading mode and bone cell activity. Further work is ongoing to better understand the relationship between local strains and pore morphology.

SIGNIFICANCE & CLINICAL RELEVANCE: This work is the first step towards developing a structure-function relationship for cortical bone that may be used as a normative assessment of bone morphology, and help diagnosis compromised pore structure prior to fracture with the hopes of enabling earlier interventions. The inclusion of novel measures of pore morphology from other fields may reshape our understanding of cortical bone structure and mechanical function.

REFERENCES: 1. Manandhar+ *J Biomech* 2023. 2. Uniyal+ *JMBBM* 2021. 3. Bayraktar+ *J Biomech* 2004. 4. Dong+ *J Biomech* 2004. 5. Watcher+ *Bone* 2002. 6. Perilli+ *Calcif Tissue Int* 2015. 7. Mandair+ *J Biomech* 2022. 8. Schlickewei+ *J Ortho Res* 2023. 9. Kersh+ *JBMR* 2018. 10. Tsugawa+ *Scientific Reports* 2022. 11. Antonova+ *Contemp Prob of Eco* 2020. 12. Op Den Buijs+ *Ann of Biomech Eng* 2005. 13. Lee+ *J App Phys* 2013. 14. Ando+ *Bulletin of the SSA* 2009. 15. Jast+ *Ost Int* 2013. 16. Schneider+ *JBMR* 2007. 17. Frost+ *The Anat Record* 1990. 18. Bakalova+ *JBMR* 2018.

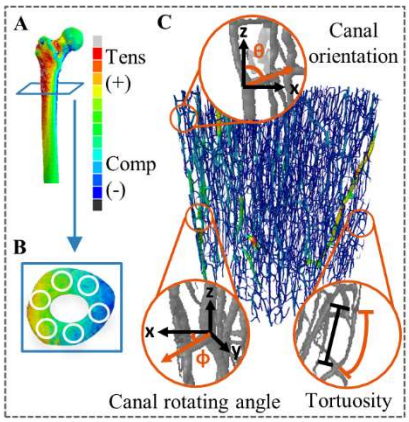

Figure 1. (A) Principal strains in the femur during walking. (B) Proximal femur cross section used as a sample extraction map. (C) Visualization of the skeletonized pore morphology from the μCT scan with key measure definitions shown

Table 1. Classical and alternative measures in regions of the femoral diaphysis habitually loaded in tension and compression during walking.

Classical measures	Tension	Compression
Median canal orientation (<Ca.θ>)	**36.36 (5.8)**	**27.82 (2.2)**
Median canal tortuosity (<Ca. τ>)	**1.074 (0.002)**	**1.072 (0.004)**
Prevalence of large pores (relCt.Po$_{100}$)	*0.31 (0.07)*	*0.20 (0.17)*
Porosity	25.7 (7.0)	22.1 (8.4)
Median canal length	0.12 (0.01)	0.13 (0.03)
Canal density	51.1 (15.6)	53.6 (18.0)
Alternative measures	**Tension**	**Compression**
Median abs. dev. canal rotating angle (MADCa.φ)	**89.76 (14.1)**	**76.89 (8.3)**
Median bifurcation angle	71.6 (3.0)	70.8 (3.7)
Median haversian length	0.14 (0.02)	0.16 (0.04)
Median volkmann length	0.1 (0.01)	0.1 (0.02)
Volkmann density	22.2 (7.9)	18.2 (5.5)
Volkmann:haversian diameter ratio	1.16 (0.12)	1.10 (0.04)

Values are mean (SD). Significant p-values ($p < 0.05$) are shown in bold. Trending p-values ($0.12 < p < 0.05$) are shown in italics.

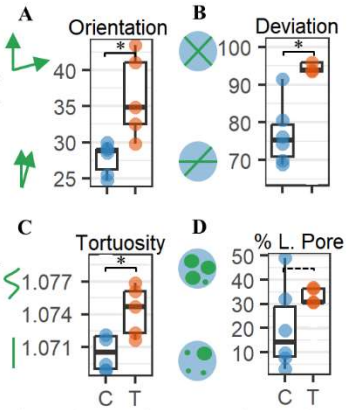

Figure 2. Box plots comparing regions of compression and tension for (A) median canal orientation, (B) MAD canal orientation, (C) median canal tortuosity, and (D) prevalence of large pores (* = $p < 0.05$, dashed = trending).